https://doi.org/10.3311/PPci.45124
Creative Commons Attribution

Periodica Polytechnica Civil Engineering

Adhesive Bond and Tensile Performance of Scrap Inner Tube Rubber for Low-cost Seismic Base Isolation in Rural Housing

Harsono Harsono[1], Tavio Tavio[1*], Gabriele Milani[2], Dinis Pinto[3], Andrew Hartanto Jusuf[1], Halid Wamala[1]

[1] Department of Civil Engineering, Faculty of Civil, Planning, and Geo Engineering, Institut Teknologi Sepuluh Nopember, Jl. Taman Alumni, Civil Engineering Building, ITS Campus, Keputih, Sukolilo, Surabaya 60111, Indonesia
[2] Department of Architecture, Built Environment and Construction Engineering, Politecnico di Milano, Piazza Leonardo da Vinci 32, 20133 Milan, Italy
[3] Department of Civil Engineering, Faculty of Engineering, Universidade da Paz, Rua Osindo 1, Manleuana, Dili, Timor-Leste
* Corresponding author, e-mail: tavio@its.ac.id

Received: 14 June 2026, Accepted: 02 November 2026, Published online: 17 November 2026

Abstract

This study evaluated the adhesive bond and tensile response of scrap inner tube rubber as a preliminary material candidate for low-cost seismic isolation. Ten single-lap specimens bonded with a solvent-based polychloroprene adhesive were tested using a comparative joint configuration adapted from ASTM D1002: five untreated control specimens (CS) and five mechanically roughened specimens (RS). Using the confirmed bonded area of 322.58 mm^2, surface roughening increased the average apparent lap-shear strength from 0.064 MPa to 0.167 MPa and the average failure displacement from 51.7 mm to 182.4 mm. Welch two-sample tests confirmed clear differences in apparent strength (mean difference 0.1029 MPa, 95% CI 0.0944–0.1113 MPa) and displacement (mean difference 130.7 mm, 95% CI 121.0–140.4 mm), both $p < 0.001$. Roughening also shifted joint failure from predominantly interfacial separation toward cohesive or mixed patterns. Five dumbbell rubber specimens were tested under uniaxial loading with reference to ASTM D412 Die C. The rubber reached an average tensile stress of 7.07 MPa and sustained an average crosshead displacement of 331 mm before rupture; elongation at break was not determined because no extensometer was used. These coupon-scale results establish preliminary material and joint feasibility; cyclic compression-shear, durability, process-control, source-variability, and component-level testing remain necessary.

Keywords

base isolation, polychloroprene adhesive, recycled inner-tube rubber, resource efficiency, surface roughening

1 Introduction

Low-cost seismic isolation is an important strategy for improving earthquake resilience in regions where conventional isolators are economically difficult to implement. Rural housing in earthquake-prone areas can benefit from isolation systems that reduce transmitted acceleration and interstory drift, while locally available recycled rubber offers a potentially accessible material base [1, 2]. Recycled-rubber isolation devices have shown encouraging responses in shaking-table tests and analytical studies, including reductions in roof acceleration, interstory drift, and seismic demand [3, 4].

Recycled rubber bearings and fiber-reinforced elastomeric isolators can be fabricated using rubber matrices, reinforcement layers, and either heat-activated or cold adhesive bonding. Previous studies have reported promising cyclic compression and shear characteristics of recycled-rubber and fiber-reinforced bearings [5, 6]. Meanwhile, recent work has examined mechanical property enhancement, shaking table validation, and response control using recycled rubber or hybrid damping devices [7–9]. Several related systems have also been proposed, including stacked scrap tire pads, granular-rubber isolator elements, and soil-filled tire systems [10–16].

The behavior of scrap tire pad systems has been widely discussed; however, scrap inner-tube rubber remains less explored. Inner-tube rubber differs from tire tread rubber in terms of composition, thickness, previous service history, and surface condition; therefore, its adhesive and tensile properties cannot be assumed to match those of outer tire rubber. Indonesian low-cost rubber and fiber-reinforced

Cite this article as: Harsono, H., Tavio, T., Milani, G., Pinto, D., Jusuf, A. H., Wamala, H. "Adhesive Bond and Tensile Performance of Scrap Inner Tube Rubber for Low-cost Seismic Base Isolation in Rural Housing", Periodica Polytechnica Civil Engineering, 2026. https://doi.org/10.3311/PPci.45124

isolator studies have shown that tensile response, hyperelastic behavior, rubber hardness, reinforcement type, and isolator configuration must be characterized before practical base isolation applications [17–24].

For laminated rubber isolation concepts, two local material characteristics are especially important: the tensile extensibility of the rubber layer and the integrity of the adhesive bonds between the rubber sheets or between the rubber and reinforcement. Conventional elastomeric bearings perform well but may be expensive and heavy, whereas recycled rubber offers a low-cost solution only if the variability, bond durability, and cyclic behavior are controlled [25–29]. Single-lap testing can screen bonded-joint performance, but the measured response is an apparent joint property influenced by overlap geometry, adherend flexibility, eccentricity, peel stress, and surface preparation [30–32].

Accordingly, this study is positioned as a preliminary material- and joint-screening investigation rather than validation of a complete seismic isolator. Its specific contribution is the combined characterization of an underexplored recycled rubber source (scrap inner tube rubber) and its bonded interface before device fabrication. The objectives are to quantify the influence of a simple, reproducible mechanical roughening treatment on apparent lap-shear strength and failure displacement, assess repeatability and joint failure patterns, measure tensile stress and crosshead displacement at break, and benchmark the results against published recycled and isolation-related elastomers. The resulting data define both the potential and additional qualification required before cyclic or isolator-level application.

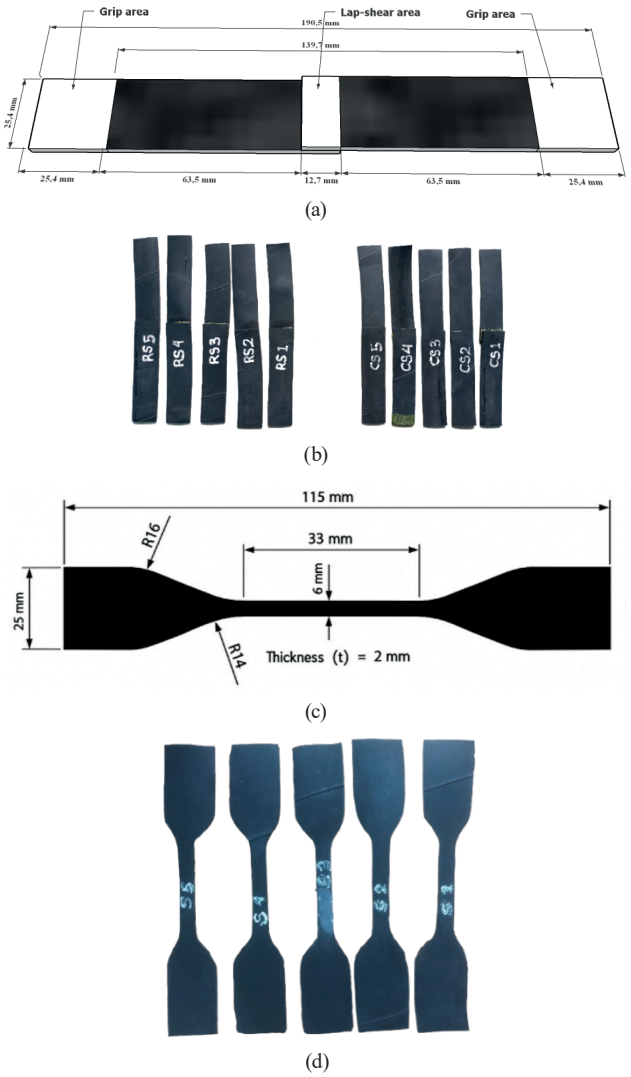


Fig. 1 Specimen geometry and material preparation details. (a) Enlarged lap-joint dimensions, (b) representative roughened specimens (RS, left) and untreated control specimens (CS, right), (c) enlarged dumbbell tensile specimen dimensions, and (d) dumbbell tensile specimens

2 Materials and methods

2.1 Materials and specimen preparation

The experimental program consisted of adhesive single-lap testing and tensile testing of scrap inner tube rubber, as summarized in Table 1 and illustrated in Fig. 1. The rubber sheets had a nominal thickness of approximately 2 mm. For the bonded specimens, the joint geometry and loading concept were adapted from ASTM D1002 for a controlled comparison between surface treatments; full compliance is not claimed because ASTM D1002 is intended for metal-to-metal bonded joints [33]. As shown in Fig. 1(a), the specimen width was 25.4 mm, and the overlap length was 12.7 mm, giving a nominal bonded area of 322.58 mm^2. Two surface conditions were considered: untreated control specimens (CS) and mechanically roughened specimens (RS). Surface roughness and adhesive-layer thickness are known to affect the apparent single-lap response [34].

Table 1 Experimental program and specimen groups

Test	Specimen group	Number	Main output
Single-lap shear	CS: untreated surface	5	Maximum load, apparent lap–shear strength, displacement, and failure mode
Single-lap shear	RS: roughened surface	5	Maximum load, apparent lap–shear strength, displacement, and failure mode
Tensile	S1–S5 dumbbell specimens	5	Tensile stress, crosshead displacement at break, and fracture mode

Tensile specimens were cut using a metal mold according to the geometry shown in Fig. 1(c), with reference to ASTM D412 Die C [35], and contained no adhesive joints. The preparation tools and testing equipment are shown in Fig. 2.

The specimen preparation followed a consistent sequence. Prior to bonding, the rubber surfaces were cleaned with acetone. In the RS group, the surface roughening process was manually performed solely within the designated bonding area on both the inner and outer surfaces of the inner-tube material, utilizing a hacksaw blade with 24 teeth per inch. The blade was moved back and forth approximately 25 times under consistent manual handling until a visually uniform roughened surface was obtained. Therefore, a sandpaper grit designation was not applicable to the roughening procedure. After roughening, the treated surfaces were cleaned again with acetone before adhesive application. Representative photographs of the rubber surface before and after the roughening treatment are presented in Fig. 3, illustrating the visual change in the surface texture produced by the procedure.



(a)



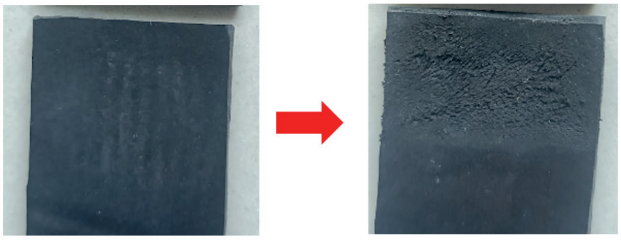
(b)

(c)

Fig. 2 Materials and testing equipment (a) scrap inner tube rubber and preparation tools; (b) universal testing machine used for adhesive lap-shear test; (c) universal testing machine used for tensile test

The adhesive used was 3M™ Neoprene High Performance Rubber & Gasket Adhesive 1300L, a solvent-based polychloroprene adhesive. It was applied to one side of the adherend surfaces using a brush. Spot measurements of the resulting bondline were generally on the order of 0.1 mm, with some readings below 0.1 mm; therefore, 0.1 mm is treated as a representative rather than a controlled uniform thickness. The adhesive was allowed to stand for approximately 4 min at room temperature before joining. After assembly, a thin hollow steel section was placed over the specimens to distribute the load, and adhesive cans were used as dead weights. The applied mass and resulting contact pressure were not measured and are therefore not reported quantitatively. The bonded specimens were cured at room temperature for approximately 168 h (7 days) before testing. Manufacturer technical data (typical values) for the adhesive are summarized in Table 2.

The roughening procedure was intentionally simple and compatible with basic workshop tools. For small specimen batches, manual abrasion has low equipment requirements, but its labor demand and operator variability become important at a larger scale. Therefore, a future production process should replace subjective visual roughness control with a mechanized abrasive wheel, belt, or roller



(a) (b)

Fig. 3 Representative photographs of the rubber surface before and after roughening: (a) before roughening and (b) after roughening

Table 2 Technical specifications of the adhesive used in this study

Property	Specification / Value
Commercial product/base	3M™ Neoprene High Performance Rubber & Gasket Adhesive 1300L / polychloroprene
Color	Yellow
Solids content by weight	26–33%
Viscosity	250–1000 cP at 27 °C (80 °F)
180° peel adhesion (168 h, 23 °C)	832 oz/in (canvas-to-steel)

operated at a specified feed rate, contact force, and number of passes, followed by quantified surface-roughness verification. No time-motion or cost study was performed in the present work; therefore, the cost effectiveness of scaled fabrication cannot be claimed quantitatively.

2.2 Testing procedures

Single-lap tests were conducted using a universal testing machine (UTM) at a displacement rate of 50 mm/min. One specimen end was fixed, and the opposite end was loaded monotonically until separation or failure. Load–displacement data were recorded continuously. The joint configuration was used as a comparative screening test rather than a pure shear material test. The apparent was calculated from the maximum recorded load using lap–shear strength Eq. (1).

$$\tau_{app} = \frac{P_{max}}{A_o}, \quad (1)$$

where τ_{app} is the apparent lap-shear strength (MPa), P_{max} is the maximum load (N), and A_o is the nominal bonded overlap area, equal to 25.4 mm × 12.7 mm = 322.58 mm^2 for all specimens. Because the single-lap geometry is eccentric and the rubber adherends are flexible, the nominal stress is non-uniform and may contain increasing peel/tensile components as the joint rotates. Joint rotation was not instrumented in the present tests; consequently, the reported values are comparative apparent stresses/strengths, not intrinsic adhesive shear properties. Failure modes were interpreted using adhesive, cohesive, and mixed terminology with reference to ASTM D5573 [36].

Failure mode classification was used as a qualitative quality-control indicator in addition to the measured strength. Adhesive failure denotes separation mainly at the adhesive-rubber interface, cohesive failure denotes damage within the adhesive or adjacent rubber, and mixed failure denotes combined interfacial and material damage. The post-test photographs were not acquired with calibrated planimetric imaging; therefore, percentage adhesive/cohesive failure areas could not be reconstructed reliably, and no retrospective area fractions were reported.

Tensile tests were performed at a displacement rate of 100 mm/min until rupture. These specimens were cut from the scrap inner tube rubber only and contained no adhesive or bonded interface. The dumbbell geometry was based on the ASTM D412 Die C-type dimensions shown in Fig. 1(c) [35], with a reduced-section length of 33 mm. A dedicated extensometer was not used, so the strain in the reduced section could not be measured directly. The UTM crosshead displacement was therefore recorded as the deformation measure. Because the crosshead displacement also includes the deformation of the transition and gripped regions, it cannot be converted into a standard elongation at break, and elongation at break is not reported in this study. The measured outputs were the engineering tensile stress, the crosshead displacement at break, and the corresponding stress–crosshead displacement response. Failure locations and fracture surfaces were inspected to distinguish reduced-section failures from grip-related failures, while necking, microcrack development, and tearing were recorded as qualitative indicators of elastomeric damage evolution [37].

The tensile results were also examined for the location of specimen rupture relative to the grips. Rupture within the reduced section is preferable to failure at a grip because the latter may be affected by clamping damage or local stress concentration. However, the present test records do not provide local strain measurements, and the recorded stress–crosshead displacement response must not be described as a measured stress–strain curve.

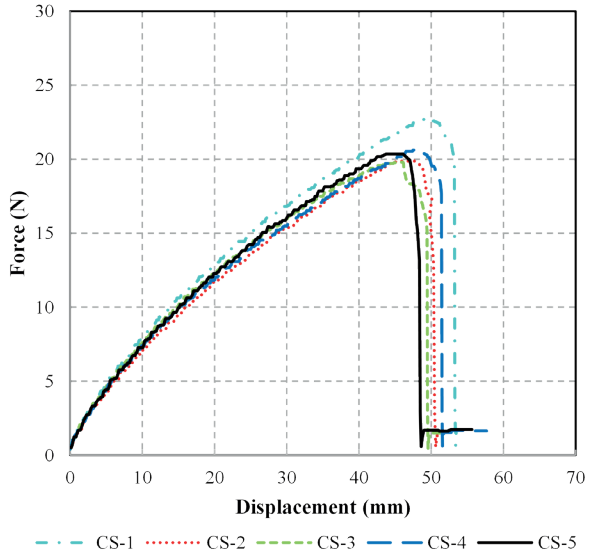
3 Results and discussion

3.1 Lap–shear load-displacement response

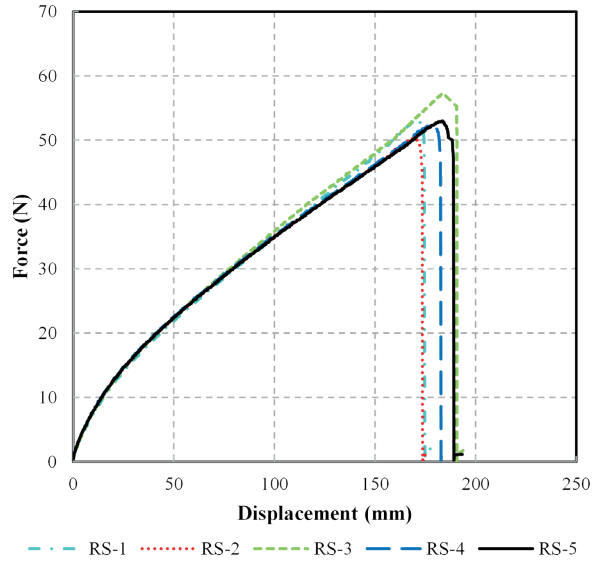
The load-displacement responses in Fig. 4(a) and 4(b) show that both groups developed increasing loads with increasing displacement until joint failure. The roughened RS specimens reached substantially higher peak loads and larger failure displacements than the untreated CS specimens. The average failure displacement increased from 51.7 mm for CS to 182.4 mm for RS, corresponding to an increase of approximately 253%. Because the engineering comparison is based on the nominal bonded stress, the corrected stress values calculated with the confirmed 322.58 mm^2 overlap area are presented in Section 3.2 and Table 3.

The improvement is consistent with increased interfacial contact and mechanical interlocking produced by surface roughening. Similar trends have been reported for bonded joints, in which surface morphology and adhesive selection govern joint strength [38, 39]. The present result is nevertheless specific to the adopted flexible-rubber single-lap geometry and should not be interpreted as a transferable intrinsic adhesive property.

The two groups differed primarily in peak capacity and the displacement reached before separation. The untreated specimens lost capacity shortly after peak load, consistent with premature interfacial debonding. The roughened specimens reached substantially larger displacement



(a)



(b)

Fig. 4 Force–displacement response of lap–shear specimens. (a) Untreated control specimens; (b) roughened specimens

before separation, although the final post-peak load drop remained relatively abrupt. Therefore, the monotonic curves support improved resistance to interface separation and greater failure displacement, but they do not establish stable cyclic ductility.

For laminated isolation concepts, the combined increase in the apparent joint strength and failure displacement is relevant because the bonded layers must transfer stress while accommodating deformation. However, earthquake loading is cyclic and occurs together with sustained vertical compression; the present monotonic comparison provides only a screening-level indication of the interface quality.

3.2 Apparent lap–shear strength

The apparent lap-shear stress–displacement response in Fig. 5 follows the same trend as the load–displacement curves. By recalculating with the verified bonded area of 322.58 mm^2, the average apparent lap–shear strength was determined to be 0.064 MPa for the CS specimens and 0.167 MPa for the RS specimens as shown in Table 3. This

Table 3 Apparent lap-shear strength and failure displacement of single-lap specimens

Specimen ID	Apparent lap-shear strength (MPa)	Displacement (mm)
CS-1	0.071	53.5
CS-2	0.064	51.0
CS-3	0.060	49.6
CS-4	0.063	51.6
CS-5	0.061	52.6
Average	0.064	51.7
SD	0.004	1.49
CoV	6.3%	2.9%
RS-1	0.165	174.8
RS-2	0.159	173.9
RS-3	0.178	190.7
RS-4	0.166	183.0
RS-5	0.167	189.4
Average	0.167	182.4
SD	0.007	7.88
CoV	4.1%	4.3%

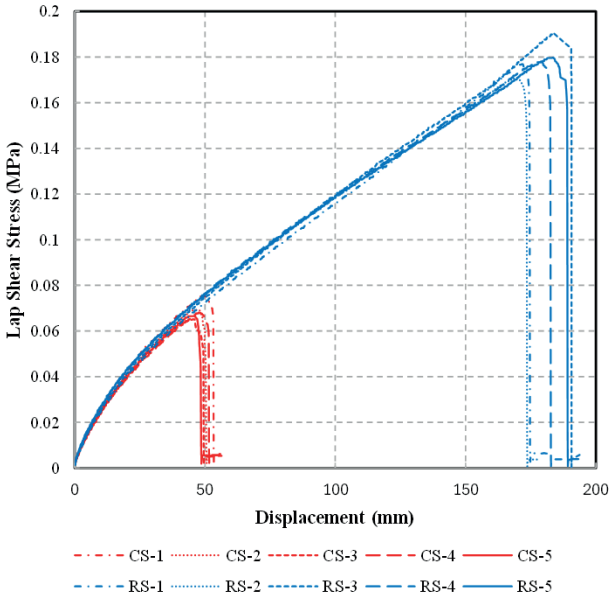


Fig. 5 Apparent lap-shear stress–displacement curves of untreated and roughened single-lap specimens; the maximum stress on each curve is reported as the apparent lap-shear strength

represents an increase of approximately 161%. The maximum values were 0.071 MPa for CS and 0.178 MPa for RS, respectively. The coefficients of variation were low in both groups.

The calculated values are comparative bonded-joint indicators under the adopted geometry rather than intrinsic adhesive material constants. This distinction is particularly important for flexible rubber adherends, for which eccentricity and large rotation can progressively change the loading from nominal shear to mixed shear-peel/tension. ASTM D1002 was selected because it provides a simple, repeatable single-lap screening geometry for isolating the effect of surface preparation with the available equipment. Comparative studies also show that the lap-joint configuration and test method materially influence the measured apparent response [40, 41]; therefore, future work should include peel/block-shear or other flexible-adherend joint tests and cyclic bonded-joint loading.

A quantitative adhesive-to-rubber stiffness ratio could not be reported because the cured adhesive modulus was not measured. The same joint geometry, adhesive application sequence, cure duration, and loading configuration were nevertheless applied to both the CS and RS groups, so that the relative effect of the surface treatment remains directly comparable. Any future qualification program should measure the adhesive thickness and cured modulus and instrument joint rotation so that local mixed-mode stresses can be quantified.

The coefficients of variation in Table 3 were low within each group. To quantify group separation, Welch's two-sample t-tests were applied because equal variances were not assumed. For apparent lap-shear strength, the CS mean was 0.0640 MPa (SD 0.0040; 95% CI 0.0590–0.0690 MPa), and the RS mean was 0.1668 MPa (SD 0.0068; 95% CI 0.1584–0.1753 MPa); the mean difference was 0.1029 MPa (95% CI 0.0944–0.1113 MPa), $t = 29.15$, $d_f = 6.50$, $p < 0.001$. For failure displacement, the CS mean was 51.66 mm (SD 1.50; 95% CI 49.80–53.52 mm) and the RS mean was 182.36 mm (SD 7.88; 95% CI 172.58–192.14 mm); the mean difference was 130.70 mm (95% CI 121.00–140.40 mm), $t = 36.45$, $d_f = 4.29$, $p < 0.001$. These tests confirmed that the very large observed differences were readily detectable; however, $n = 5$ per group remains too small to characterize the distribution shape or provide strong sensitivity to small or moderate effects; statistical inference should therefore be interpreted together with the effect size and the limited experimental scope.

3.3 Failure modes of adhesive joints

The representative post-test surfaces are shown in Fig. 6. Across the CS group, the observed response was dominated by interfacial separation, whereas the RS group more frequently showed adhesive residue on both surfaces and local substrate damage consistent with cohesive or mixed behavior. This group-level interpretation is based on the complete set of specimens rather than assigning a definitive failure class to an individual cropped photograph.

The shift is consistent with the improved adhesive-rubber interaction after roughening; however, the evidence remains qualitative. Because calibrated plan-view photographs and image-analysis thresholds were not recorded, the percentages of adhesive, cohesive, and mixed failure area could not be quantified retrospectively. Future joint tests should photograph both fracture surfaces normal to the plane with a scale and controlled illumination so that failure-area fractions can be measured reproducibly.

3.4 Tensile stress-crosshead displacement behavior

The stress-crosshead displacement curves in Fig. 7(a) show that the scrap inner-tube rubber exhibited very large uniaxial deformation before rupture. The average tensile stress at break was 7.07 MPa, and the average crosshead displacement at break was 331 mm, as shown in Table 4. No extensometer was used in the tensile tests (Section 2.2), so the strain in the 33 mm gauge section could not be measured directly. The crosshead displacement also includes deformation of the transition and gripped regions of the dumbbell specimen. Normalizing it by the 33 mm gauge length would therefore overestimate the elongation at break, and the relationship between the two quantities is nonlinear. For this reason, elongation at break is not reported, and the crosshead displacement is presented only as a machine-based measure of deformation capacity.

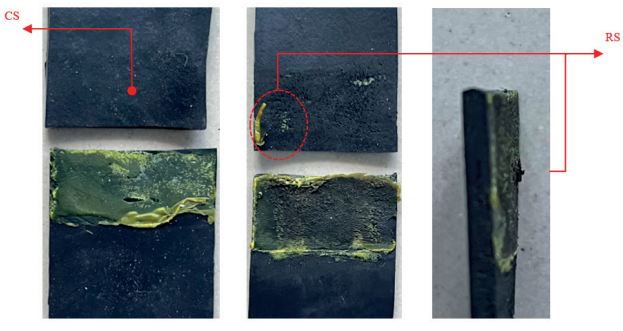
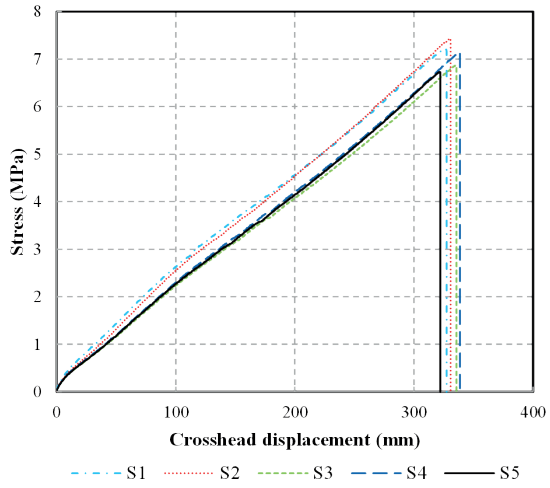
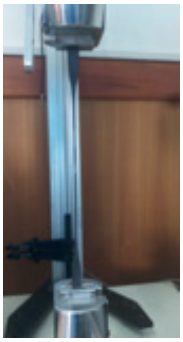


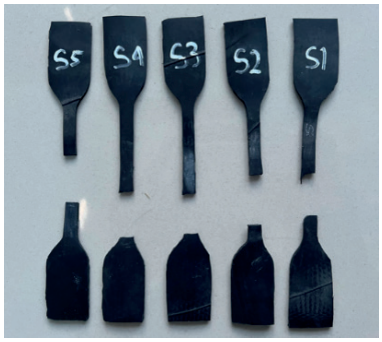
Fig. 6 Representative post-test failure surfaces following single-lap testing: (a) CS specimen showing predominantly interfacial separation; (b) and (c) RS specimens showing adhesive residue and cohesive/mixed damage



(a)



(b)



(c)

Fig. 7 Tensile response and rupture modes. (a) Stress-crosshead displacement curves, (b) necking during tensile loading, and (c) fractured tensile specimens

Table 4 Tensile stress and crosshead displacement at break of dumbbell specimens

Specimen ID	Tensile stress (MPa)	Crosshead displacement at break (mm)
S1	7.21	327
S2	7.42	331
S3	6.87	336
S4	7.14	339
S5	6.73	322
Average	7.07	331
SD	0.277	6.5
CoV	3.9%	2.0%

Note: Displacement is the UTM crosshead travel, not the extension of the 33 mm reduced section. No extensometer or other local strain measurement was used; thus, a standard-comparable elongation at break was not determined

All tensile specimens were unbonded rubber coupons and contained no adhesive joints. Rupture occurred after pronounced extension and local necking/tearing, as illustrated in Fig. 7(b–c).

The mean crosshead displacement at break was 331 mm for the tested post-service rubber specimens. This value describes the machine-recorded travel during the specified test configuration; it is not a gauge-section strain or a material elongation at break. Material composition, prior aging, formulation, and service history can affect the tensile response of rubber [42, 43]; consequently, the strength data should be regarded as source-specific rather than representative of all scrap inner tubes. The benchmarking in Section 3.5 therefore compares tensile strength only, not elongation.

For seismic-isolation development, a large deformation capacity can provide a deformation reserve, but tensile strength and deformation capacity alone do not establish suitability, because an isolator is primarily governed by cyclic shear under sustained compression, together with stability, damping, aging, and interface integrity. Therefore, the present tensile data are benchmarked in Section 3.5 and used only as screening parameters for future layer and prototype design.

The tensile test was monotonic and uniaxial, whereas the laminated isolator experiences repeated multiaxial loading. Therefore, the crosshead displacement at break must not be converted into an allowable isolator shear strain. Instead, the material must be qualified at the compound, bonded laminate, and full-component scales.

3.5 Benchmarking and engineering implications

Table 5 compares the measured tensile strength of the present scrap inner-tube rubber with selected recycled and isolation-related elastomer compounds. At 7.07 MPa, the mean tensile stress at break exceeded the values reported for the recycled tire-particle matrix of Meza-Muñoz et al. [15], the ground-tire-rubber/butyl compound of Formela and Haponiuk [44], and the reclaimed rubber compound of Cilento et al. [45]. By contrast, Pianese et al. [46] reported a tensile strength of 16.06 MPa for a high-damping natural-rubber/EPDM compound investigated for an unbonded fiber-reinforced elastomeric isolator (UFREI). These comparisons concern tensile strength alone: the present

Table 5 Benchmark tensile strength of the tested scrap inner tube rubber and selected literature materials

Material/source	Tensile strength (MPa)
Scrap inner tube rubber, present study	7.07
Recycled tire-particle matrix [15]	2.45–3.13
Butyl rubber + 30 phr GTR [44]	2.68
Reclaimed rubber compound [45]	2.60
High-damping NR-EPDM blend [46]	16.06

experiment did not determine gauge-section elongation at break, so no relative ranking of elongation or extensibility is justified. Fiber-reinforced neoprene isolators have also been studied [47], but their device-level performance is not directly comparable with the present material and bonded-joint coupons.

Table 5 excludes elongation at break because no gauge-section extensometry or equivalent local strain measurement was available (Section 2.2). The high-damping compound study [46] discusses UNI EN 15129 minimum tensile properties of 12 MPa tensile strength and 400% elongation at break for its relevant elastomer category. The present 7.07 MPa tensile result is below that cited strength benchmark, and compliance with the elongation benchmark cannot be assessed. The present coupons consequently do not establish compliance with isolation-grade elastomer requirements; the applicability of any particular material specification would need to be determined for the proposed isolator design.

Likewise, there is no universal single-lap coupon strength threshold that qualifies a laminated seismic isolator. The measured 0.167 MPa apparent lap–shear strength of the roughened joints is therefore used as a fabrication screening metric, not an allowable design stress.

From a fabrication viewpoint, manual roughening remains attractive for laboratories or very small-scale rural production because it requires only simple tools. However, at a larger scale, repeatability, labor time, dust/debris control, and surface-quality verification become part of the cost equation. Therefore, a mechanized surface preparation step with measurable roughness targets should be evaluated before any claim of scalable cost advantage.

3.6 Limitations and qualification pathway

The present study was a monotonic coupon-scale screening program. It did not evaluate cyclic deformation, sustained vertical compression, compression-shear interaction, creep, temperature variation, moisture/ozone exposure, aging, or full-bearing instability. ISO 22762-1:2024 distinguishes rubber-material tests from tests of elastomeric isolator characteristics [48]; therefore, the results do not demonstrate that an isolator made from this material would meet seismic isolation qualification requirements.

The small sample size ($n = 5$ per group) and single scrap source limit generalizability. Future studies should test several inner tube sources and record their origin, thickness, hardness, aging condition, and formulation indicators, so that between-source variability can be separated from test repeatability. In addition, the tensile tests were performed without an extensometer, so standard elongation at break could not be determined; future tensile tests should use contact or non-contact (video) extensometry.

Process control also requires improvement. Although the adhesive product and its technical data are documented and spot bondline measurements were generally around 0.1 mm, the bondline thickness was not uniformly controlled, and the dead-weight contact pressure was not measured. Future bonded-joint studies should record the adhesive batch, specimen-specific bondline thickness, open time, contact pressure, cure conditions, cured adhesive modulus, quantitative surface roughness (e.g., Ra and Rz), and treatment time. Parameters not measured in the present campaign are not reconstructed retrospectively.

A staged qualification program is recommended: (i) repeat coupon tests with quantified surface, adhesive, and strain-measurement variables; (ii) cyclic bonded-joint and peel/mixed-mode tests suitable for flexible adherends; (iii) laminated coupon or subcomponent tests under compression-shear and environmental conditioning; and (iv) full prototype isolator tests for vertical and effective horizontal stiffness, equivalent damping, recentering, residual deformation, delamination, rollover/buckling stability, and cyclic property degradation.

Within these boundaries, the data support only preliminary feasibility: mechanical roughening produced a large and statistically clear improvement in the single-lap response, and the tested rubber sustained large deformation before rupture. The study thus provides material-screening evidence and a direction for process refinement, while structural applicability remains to be demonstrated at the component scale.

4 Conclusions

This study characterized scrap inner tube rubber and its polychloroprene-bonded interface as a preliminary input for low-cost laminated seismic isolation development. Using the confirmed 322.58 mm^2 bonded area, mechanical roughening increased the average apparent lap-shear strength from 0.064 MPa to 0.167 MPa and the average failure displacement from 51.7 mm to 182.4 mm. Welch tests confirmed that the group differences were large relative to within-group scatter ($p < 0.001$), although only five specimens were tested per group. Roughening also shifted the group-level failure observations from predominantly interfacial separation toward cohesive or mixed

patterns. The unbonded rubber tensile coupons reached 7.07 MPa average tensile stress and sustained a large average crosshead displacement of 331 mm before rupture. Because no extensometer was used, standard elongation at break could not be determined. Benchmarking indicates a higher tensile strength than several published recycled-rubber compounds, but a lower tensile strength than a representative engineered high-damping NR-EPDM isolator compound and the 12 MPa minimum cited for isolation-grade high-damping elastomers. The findings therefore establish coupon-scale material and joint feasibility, not seismic-isolator suitability. Extensometer-based tensile testing, cyclic compression-shear testing, quantified surface/adhesive process control, environmental durability, source-variability assessment, and full-component qualification are required before structural application.

Acknowledgement

This research was funded by the Indonesian Endowment Fund for Education (LPDP) on behalf of the Indonesian Ministry of Higher Education, Science, and Technology, and managed under the EQUITY Program (Contract Nos. 4299/B3/DT.03.08/2025 and 3029/PKS/ITS/2025). The authors gratefully acknowledge financial support from the Institut Teknologi Sepuluh Nopember under the Publication Writing and IPR Incentive Program (PPHKI) 2026.

References

[1] Losanno, D., Ravichandran, N., Parisi, F. "Seismic fragility of base-isolated single-storey unreinforced masonry buildings equipped with classical and recycled rubber bearings in Himalayan regions", Journal of Building Engineering, 45, 103648, 2022. https://doi.org/10.1016/j.jobe.2021.103648

[2] Tavio, Wijaya, U. "Experimental study of Indonesian low-cost glass fiber reinforced elastomeric isolators (GFREI)", International Journal on Advanced Science, Engineering and Information Technology, 10(1), pp. 311–317, 2020. https://doi.org/10.18517/ijaseit.10.1.8054

[3] Losanno, D., Spizzuoco, M., Calabrese, A. "Bidirectional shaking-table tests of unbonded recycled-rubber fiber-reinforced bearings (RR-FRBs)", Structural Control and Health Monitoring, 26(9), e2386, 2019. https://doi.org/10.1002/stc.2386

[4] Siow, Y. T., Kasa, A., Osman, S. A. "Recycled tire isolator as earthquake resistance system for low-rise buildings", Malaysian Journal of Civil Engineering, 26(1), pp. 51–61, 2014. https://doi.org/10.11113/mjce.v26.15875

[5] Rofiq, H. I., Tavio, Iranata, D. "Model validation of carbon-fiber and glass-fiber reinforced elastomeric isolators using finite element method", IOP Conference Series: Earth and Environmental Science, 1116(1), 012001, 2022. https://doi.org/10.1088/1755-1315/1116/1/012001

[6] Putra, G. N. A. W., Tavio, Iranata, D. "Comparative mechanical behavior of low-cost flax fiber reinforced elastomeric isolator (FREI) with shape variation", Civil Engineering and Architecture, 12(1), pp. 15–25, 2024. https://doi.org/10.13189/cea.2024.120102

[7] Rivas-Ordonez, F. S., Meza-Munoz, A. O., Madera-Sierra, I. E., Rojas-Manzano, M. A., Patino, E. D., Salmerón-Becerra, M. I., Dyke, S. J. "Alternatives for enhancing mechanical properties of recycled rubber seismic isolators", Polymers, 16(16), 2258, 2024. https://doi.org/10.3390/polym16162258

[8] Calabrese, A., Spizzuoco, M., Serino, G., Della Corte, G., Maddaloni, G. "Shaking table investigation of a novel, low-cost, base isolation technology using recycled rubber", Structural Control and Health Monitoring, 22(1), pp. 107–122, 2015. https://doi.org/10.1002/stc.1663

[9] Maddaloni, G., Caterino, N., Occhiuzzi, A. "Shake table investigation of a structure isolated by recycled rubber devices and magnetorheological dampers", Structural Control and Health Monitoring, 24(5), e1906, 2017. https://doi.org/10.1002/stc.1906

[10] Singh, P. K., Singh, B., Chakravarty, S. "Performance of base isolator from scrap tyre rubber pads on building", International Journal of Engineering Research & Technology, 11(6), pp. 45–49, 2022. https://doi.org/10.5281/zenodo.18440269

[11] Kodanda Pavan Sai, P., Prasad, J. S. R., Kumar Balguri, P. "Analysis of scrap tyre rubber pad base isolated structure using MATLAB", Materials Today: Proceedings, 62, pp. 2970–2974, 2022. https://doi.org/10.1016/j.matpr.2022.02.572

[12] Mathew, A., Sajeeb, R. "Seismic performance of multistoried building frames with unbonded scrap tyre pad isolators", AIJR Proceedings, pp. 190–200, 2023. https://doi.org/10.21467/proceedings.156.26

[13] Losanno, D., Ravichandran, N., Parisi, F., Calabrese, A., Serino, G. "Seismic performance of a low-cost base isolation system for unreinforced brick masonry buildings in developing countries", Soil Dynamics and Earthquake Engineering, 141, 106501, 2021. https://doi.org/10.1016/j.soildyn.2020.106501

[14] Calabrese, A., Spizzuoco, M., Strano, S., Terzo, M. "Hysteresis models for response history analyses of recycled rubber-fiber reinforced bearings (RR-FRBs) base isolated buildings", Engineering Structures, 178, pp. 635–644, 2019. https://doi.org/10.1016/j.engstruct.2018.10.057

[15] Meza-Muñoz, A. O., Rivas-Ordoñez, F. S., Madera-Sierra, I. E., Rojas-Manzano, M. A., Patino-Reyes, E. D., Salmerón-Becerra, M. I., Dyke, S. J. "Development of a matrix for seismic isolators using recycled rubber from vehicle tires", Polymers, 16(21), 2977, 2024. https://doi.org/10.3390/polym16212977

[16] Van de Lindt, J. W., Atadero, R. A. "Shake table test results for a half-scale reinforced concrete Indonesian house with and without economical base isolation", Asian Journal of Civil Engineering (Building and Housing), 9(1), pp. 1–13, 2008. [online] Available at: https://scispace.com/papers/shake-table-test-results-for-a-half-scale-reinforced-10l4gr20sr [Accessed: 24 September 2026]

[17] Raj, J. C. J., Suppiah, S. "Seismic isolation using scrap tire rubber pads", Materials Today: Proceedings, 43(2), pp. 1404–1407, 2021. https://doi.org/10.1016/j.matpr.2020.09.176

[18] Park, J., Shirai, K., Kikuchi, M. "A seismic mass damper system using scrap tire pads: Loading tests on mechanical properties and numerical assessment of the response control effects", Soil Dynamics and Earthquake Engineering, 157, 107257, 2022. https://doi.org/10.1016/j.soildyn.2022.107257

[19] Wijaya, B. T. W., Tavio "Mechanical properties of Indonesian rubber for low-cost base isolation", International Journal of Civil Engineering and Technology, 10(1), pp. 884–890, 2019. [online] Available at: https://scholar.its.ac.id/en/publications/mechanical-properties-of-indonesian-rubber-for-low-cost-base-isol/ [Accessed: 24 September 2026]

[20] Wijaya, U., Soegiarso, R., Tavio "Mechanical properties of Indonesian hyperelastic low-grade rubber for low-cost base isolator", MATEC Web of Conferences, 276, 01017, 2019. https://doi.org/10.1051/matecconf/201927601017

[21] Tavio, Wijaya, U. "Comparative behavior of local hyperelastic low-grade rubbers for low-cost base isolation", MATEC Web of Conferences, 276, 01001, 2019. https://doi.org/10.1051/matecconf/201927601001

[22] Rayendra, M., Tavio "Effect of high-damping rubber bearings on performance of high-rise buildings in highly and moderate seismic regions", In: Nia, E. M., Awang, M. (eds.) Advances in Civil Engineering Materials: Selected Articles from the 7th International Conference on Architecture and Civil Engineering, Springer, Singapore, pp. 177–187, 2024. https://doi.org/10.1007/978-981-97-0751-5_18

[23] Harsono, B., Tavio "Tensile properties of fiberglass as reinforcement of low-cost rubber base isolator for small houses", International Journal of Civil Engineering and Technology, 10(1), pp. 1933–1940, 2019. [online] Available at: https://iaeme.com/Home/article_id/IJCIET_10_01_177 [Accessed: 24 September 2026]

[24] Harsono, B., Tavio, Basori "Shaking up seismic safety: Low-cost rubber base insulator strip (LCRBI-S) improves stiffness for earthquake-resistant housing", AIP Conference Proceedings, 3167(1), 040014, 2024. https://doi.org/10.1063/5.0223355

[25] Losanno, D., Calabrese, A., Madera-Sierra, I. E., Spizzuoco, M., Marulanda, J., Thomson, P., Serino, G. "Recycled versus natural-rubber fiber-reinforced bearings for base isolation: Review of the experimental findings", Journal of Earthquake Engineering, 26(4), pp. 1921–1940, 2022. https://doi.org/10.1080/13632469.2020.1748764

[26] Thin, K. T., Garciano, L. E. O. "Development and validation of low-cost FREBs using recycled butyl rubber for seismic isolation", Structural Engineering International, pp. 1–9, 2026. https://doi.org/10.1080/10168664.2026.2615798

[27] Bafandeh Nobari, H., Akbari Hamed, A., Saeidzadeh, M. "Experimental study on the cyclic performance of novel seismic base isolators made by scrap tire rubber pads", Iranian Journal of Science and Technology, Transactions of Civil Engineering, 48, pp. 4349–4366, 2024. https://doi.org/10.1007/s40996-024-01420-x

[28] Zhang, C., Ali, A. "The advancement of seismic isolation and energy dissipation mechanisms based on friction", Soil Dynamics and Earthquake Engineering, 146, 106746, 2021. https://doi.org/10.1016/j.soildyn.2021.106746

[29] Reyna, R., Velásquez, D., Chavez, J., Zavala, C. "Experimental study of low-cost base isolation prototype (ABC) with enhanced energy dissipation", In: Proceedings of the 18th World Conference on Earthquake Engineering, Milan, Italy, 2024. [online] Available at: https://program.wcee2024.it/?id=IDD9&mode=session [Accessed: 24 September 2026].

[30] Chen, Q., Du, B., Zhang, X., Zhong, H., Ning, C., Bai, H., Li, Q., Pan, R., Zhou, B., Hu, H. "Parametric investigation into the shear strength of adhesively bonded single-lap joints", Materials, 15(22), 8013, 2022. https://doi.org/10.3390/ma15228013

[31] da Silva, L. F. M., das Neves, P. J. C., Adams, R. D., Spelt, J. K. "Analytical models of adhesively bonded joints-Part I: Literature survey", International Journal of Adhesion and Adhesives, 29(3), pp. 319–330, 2009. https://doi.org/10.1016/j.ijadhadh.2008.06.005

[32] Tsai, M. Y., Oplinger, D. W., Morton, J. "Improved theoretical solutions for adhesive lap joints", International Journal of Solids and Structures, 35(12), pp. 1163–1185, 1998. https://doi.org/10.1016/S0020-7683(97)00097-8

[33] ASTM International "ASTM D1002-10(2019): Standard test method for apparent shear strength of single-lap-joint adhesively bonded metal specimens by tension loading (metal-to-metal)", ASTM International, West Conshohocken, PA, USA, 2019. https://doi.org/10.1520/D1002-10R19

[34] Boutar, Y., Naïmi, S., Mezlini, S., da Silva, L. F. M., Hamdaoui, M., Ben Sik Ali, M. "Effect of adhesive thickness and surface roughness on the shear strength of aluminium one-component polyurethane adhesive single-lap joints for automotive applications", Journal of Adhesion Science and Technology, 30, pp. 1913–1929, 2016. https://doi.org/10.1080/01694243.2016.1170588

[35] ASTM International "ASTM D412-16(2021): Standard test methods for vulcanized rubber and thermoplastic elastomers - tension", ASTM International, West Conshohocken, PA, USA, 2021. https://doi.org/10.1520/D0412-16R21

[36] ASTM International "ASTM D5573-99(2019): Standard practice for classifying failure modes in fiber-reinforced-plastic (FRP) joints", ASTM International, West Conshohocken, PA, USA, 2019. https://doi.org/10.1520/D5573-99R19

[37] Zhu, X., Wang, S.-Q. "Mechanisms for different failure modes in startup uniaxial extension: bond (rupture-like) failure and necking", Journal of Rheology, 57(1), pp. 223–248, 2013. https://doi.org/10.1122/1.4764081

[38] Tiwari, M. M., Noormohammed, S., Sarkar, D. K., Chen, X.-G. "Effects of surface roughness parameters on the shear strength of AA 6061-T6 aluminium alloy in structural adhesive bonding applications", Journal of Adhesion Science and Technology, 38(24), pp. 4372–4390, 2024. https://doi.org/10.1080/01694243.2024.2380176

[39] Safari, A., Farahani, M., Ghabezi, P. "Experimental study on the influences of different surface treatment processes and adhesive type on the aluminum adhesive-bonded joint strength", Mechanics Based

Design of Structures and Machines, 50(7), pp. 2400–2413, 2022. https://doi.org/10.1080/15397734.2020.1777876

[40] Redmann, A., Damodaran, V., Tischer, F., Prabhakar, P., Osswald, T. A. "Evaluation of single-lap and block shear test methods in adhesively bonded composite joints", Journal of Composites Science, 5(1), 27, 2021. https://doi.org/10.3390/jcs5010027

[41] Guess, T. R., Allred, R. E., Gerstle, F. P. "Comparison of lap shear test specimens", Journal of Testing and Evaluation, 5(2), pp. 84–93, 1977. https://doi.org/10.1520/JTE10666J

[42] Abdelsalam, A. A., Araby, S., El-Sabbagh, S. H., Abdelmoneim, A., Hassan, M. A. "Effect of carbon black loading on mechanical and rheological properties of natural rubber/styrene-butadiene rubber/nitrile butadiene rubber blends", Journal of Thermoplastic Composite Materials, 34(4), pp. 490–507, 2021. https://doi.org/10.1177/0892705719844556

[43] Nanda, M., Tripathy, D. K. "Physico-mechanical and electrical properties of conductive carbon black reinforced chlorosulfonated polyethylene vulcanizates", Express Polymer Letters, 2(12), pp. 855–865, 2008. https://doi.org/10.3144/expresspolymlett.2008.100

[44] Formela, K., Haponiuk, J. T. "Curing characteristics, mechanical properties and morphology of butyl rubber filled with ground tire rubber (GTR)", Iranian Polymer Journal, 23, pp. 185–194, 2014. https://doi.org/10.1007/s13726-013-0214-7

[45] Cilento, F., Losanno, D., Piga, L. "Laboratory characterization of a reclaimed rubber compound for low-cost elastomeric isolators", In: Proceedings of the 8th International Conference on Computational Methods in Structural Dynamics and Earthquake Engineering (COMPDYN 2021), Athens, Greece, pp. 2525–2535, 2021. https://doi.org/10.7712/120121.8655.18969

[46] Pianese, G., Milani, G., Formisano, A. "Unbonded fiber reinforced elastomeric isolator (UFREI) made of high damping natural rubber blend", In: Proceedings of the 15th World Congress on Computational Mechanics and 8th Asian Pacific Congress on Computational Mechanics, Yokohama, Japan, 2022. https://doi.org/10.23967/wccm-apcom.2022.125

[47] Toopchi-Nezhad, H., Tait, M. J., Drysdale, R. G. "Lateral response evaluation of fiber-reinforced neoprene seismic isolators utilized in an unbonded application", Journal of Structural Engineering, 134(10), pp. 1627–1637, 2008. https://doi.org/10.1061/(ASCE)0733-9445(2008)134:10(1627)

[48] International Organization for Standardization "ISO 22762-1:2024 Elastomeric seismic-protection isolators - Part 1: Test methods", ISO, Switzerland, 2024. [online] Available at: https://www.iso.org/standard/89165.html [Accessed: 31 October 2026]